ROUGHNESS OF BRITTLE CRACK INTERFACES IN BUCKLING BEAM LATTICES

Bjørn Skjetne[1], Tørbjørn Helle[1] and Alex Hansen[2]
[2]Department of Chemical Engineering,
[1]Department of Physics,
Norwegian University of Science and Technology,
N-7491 Trondheim, Norway

Abstract

The roughness exponent of brittle cracks is obtained in computer simulations with a buckling beam lattice, i.e., a structurally two-dimensional lattice which is allowed to deflect out of the initial rest plane during fracture. The result obtained is then compared with that of the corresponding non-buckling lattice. The breaking thresholds are chosen randomly from two different distributions, one with a tail towards strong beams ($D < 0$) and the other with a tail towards weak beams ($D > 0$). In our model the influence buckling has on the roughness exponent is found to be very different for the two types of disorder used. When there is a tail towards weak beams, i.e., using $D = 1$, the exponent which characterizes the scaling behaviour is lowered from $\zeta = 0.87(1)$ to $\zeta = 0.79(2)$. For distributions with a tail towards strong beams, on the other hand, using $\zeta = -5$, the roughness exponent remains the same as that obtained with the non-buckling lattice, i.e., $\zeta = 0.86(2)$ as opposed to $\zeta = 0.85(2)$. This result we believe to be transient between low and moderate disorder, with a behaviour similar to that of $D = 1$ obtaining for stronger disorders $D < -5$. Our model of buckling represents a fully three dimensional problem, and the $D = 1$ result is in excellent agreement with the experimantal value of $\zeta = 0.8$ obtained for brittle fracture in three dimensions. As such it provides the first numerical verification of the universal roughness exponent observed in nature.

1 INTRODUCTION

Studies of fracture have been considered important for centuries but the acquisition of effective tools to describe fracture in disordered materials is a comparatively recent development. These tools have their origin in statistical physics and are known as lattice models [1], the most common being the random fuse model [2]. Lattice models allow complex breakdown phenomena to be studied, where the dominating feature is the interplay between a constantly evolving non-uniform stress field and a random meso-structure.

Most materials, be they natural or man-made, show some degree of deviation from a perfect structure. This will usually affect the way the material breaks under strain, and thus also the appearance of the final crack. Examples are fibrous, porous or granular media.

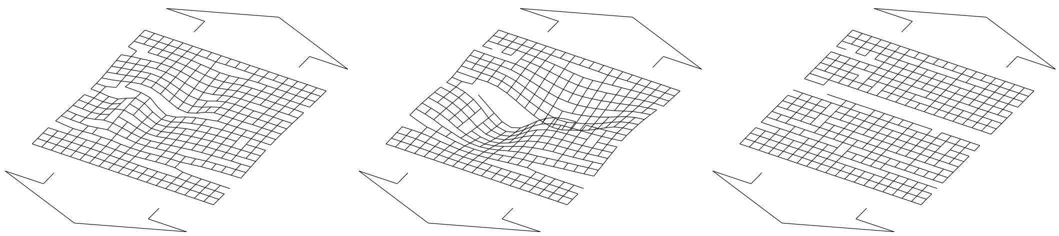

Figure 1: A lattice of size $L = 20$ showing the force couple applied uniformly on opposite edges (mode-I fracture), and the buckling which results when the lattice deviates from a perfect plane. Three stages of the fracture process are shown, i.e., where the number of beams broken are, from left to right, $N = 70$, $N = 78$ and $N = 86$.

To model such a system we use a random beam model where each beam is identical as far as the elastic properties are concerned, but with breaking thresholds chosen randomly [3, 4]. In this model disorder is regarded on a mesoscopic scale, i.e., on a scale which is much smaller than the external dimensions of the system but sufficiently large for the forces to be governed by the equations of elasticity. Presently we calculate the typical roughness value of the crack which results after a system of given size has been completely broken. The scaling behaviour is obtained by including a range of system sizes.

Scaling laws are powerful tools which relate global properties to system size, enabling the breakdown process to be analyzed in terms of a few variables. The scaling of the roughness has been found to take the form of a power law [5], i.e., $W \sim L^{\zeta}$, where the exponent ζ characterizes the asymptotic behaviour. An exponent which is independent of the details of the system signals universality in the sense that widely different systems show quantitatively the same behaviour in one or more respects. The crack roughness W is obtained from the y-variance $W^2 = \langle y_i^2 \rangle - \langle y_i \rangle^2$ of the interface, where y is the vertical coordinate from the bottom row of the lattice to the position of the crack.

Current numerical results, quoted from the literature, are $\zeta = 0.74(2)$ and $\zeta = 0.62(5)$ for the random fuse model in two [6] and three [7] dimensions, respectively, and, in the case of the (non-buckling) beam model in two dimensions [8], $\zeta = 0.86(3)$.

2 THE BUCKLING BEAM MODEL

The displacements of a real material, even if its geometry is essentially confined to a plane, will generally occupy three dimensions. For instance, when opposite forces are applied uniformly along the top and bottom edges of a sheet of paper, with the object of straining it until failure, significant displacements will be observed in the direction perpendicular to the sheet, see Fig. 1. This is especially evident in places where large cracks appear. Reasons for this behaviour are deviations in the symmetry of the material itself, or its properties, about the plane through which the externally applied forces act.

To study this behaviour, the plane beam model must include two additional features. One is the random variation of the material in the out-of-plane direction; since in the beam model the material is reduced to a set of points corresponding to the nodes on a mathematically precise two-dimensional lattice, the most convenient method of including this feature is to impose a very small randomly chosen vertical displacement on each node.

The other feature to be included is the physics of the forces which create, and maintain, the out-of-plane displacement field. In the buckling beam model we have one translational and one rotational displacement relevant to each of the principal axes, i.e., six degrees of freedom. This allows for bending moments and transverse shear forces, as well as axially tensile, or compressive, forces. For any node i there are four neighbours on the square lattice, i.e., left, right, up and down. Each time a beam is removed from the lattice, the displacement field is recalculated from

$$\sum_j D_{ij} \begin{bmatrix} u_i \\ v_i \\ w_i \\ x_i \\ y_i \\ z_i \end{bmatrix} = \lambda \begin{bmatrix} U_i \\ V_i \\ W_i \\ X_i \\ Y_i \\ Z_i \end{bmatrix}, \tag{1}$$

using the conjugate gradient method, where forces and moments are expressed as functions of displacement with respect to a coordinate system placed on each node. In contrast with the plane beam model, the coordinate system is additionally rotated about the relevant angle within the XZ-, YZ- or XY-plane, i.e., u, v or w. This is done to guard against systematic errors which would otherwise increase with increasing out-of-plane deflections.

The individual force components are then derived by considering an elastic beam with no end restraints [9], as projected onto the XY-, XZ and YZ-planes. With A, T and M denoting axial force, transverse force and bending moment, respectively, the components of Eq. (1) are

$$\begin{aligned} X_i &= {}^{\mathrm{A}}_{x}XX_i^{(1)} + {}^{\mathrm{T}}_{x}XY_i^{(1)} + {}^{\mathrm{B}}_{x}XY_i^{(1)} + {}^{\mathrm{T}}_{x}XZ_i^{(1)} + {}^{\mathrm{B}}_{x}XZ_i^{(1)} \\ &+ {}^{\mathrm{A}}_{x}XY_i^{(2)} + {}^{\mathrm{T}}_{x}XY_i^{(2)} + {}^{\mathrm{B}}_{x}XY_i^{(2)} \\ &+ {}^{\mathrm{A}}_{x}XX_i^{(3)} + {}^{\mathrm{T}}_{x}XY_i^{(3)} + {}^{\mathrm{B}}_{x}XY_i^{(3)} + {}^{\mathrm{T}}_{x}XZ_i^{(3)} + {}^{\mathrm{B}}_{x}XZ_i^{(3)} \\ &+ {}^{\mathrm{A}}_{x}XY_i^{(4)} + {}^{\mathrm{T}}_{x}XY_i^{(4)} + {}^{\mathrm{B}}_{x}XY_i^{(4)}, \end{aligned} \tag{2}$$

where the term ${}^{\mathrm{B}}_{x}XZ_i^{(1)}$, for instance, is the x-component of the buckling (B) force due to $j = 1$, as projected onto the XZ-plane. Rotational displacements about the Y- and X-axes are denoted u and v, respectively, and z is used for vertical displacements along the Z-axis. The other components of translational displacement are

$$\begin{aligned} Y_i &= {}^{\mathrm{A}}_{y}XY_i^{(1)} + {}^{\mathrm{T}}_{y}XY_i^{(1)} + {}^{\mathrm{B}}_{y}XY_i^{(1)} \\ &+ {}^{\mathrm{A}}_{y}YY_i^{(2)} + {}^{\mathrm{T}}_{y}XY_i^{(2)} + {}^{\mathrm{B}}_{y}XY_i^{(2)} + {}^{\mathrm{T}}_{y}YZ_i^{(2)} + {}^{\mathrm{B}}_{y}YZ_i^{(2)} \\ &+ {}^{\mathrm{A}}_{y}XY_i^{(3)} + {}^{\mathrm{T}}_{y}XY_i^{(3)} + {}^{\mathrm{B}}_{y}XY_i^{(3)} \\ &+ {}^{\mathrm{A}}_{y}YY_i^{(4)} + {}^{\mathrm{T}}_{y}XY_i^{(4)} + {}^{\mathrm{B}}_{y}XY_i^{(4)} + {}^{\mathrm{T}}_{y}YZ_i^{(4)} + {}^{\mathrm{B}}_{y}YZ_i^{(4)}, \end{aligned} \tag{3}$$

obtained by changing around the directions in Eq. (2), and

$$\begin{aligned} Z_i &= {}^{\mathrm{A}}_{z}XZ_i^{(1)} + {}^{\mathrm{T}}_{z}XZ_i^{(1)} + {}^{\mathrm{B}}_{z}XZ_i^{(1)} + {}^{\mathrm{A}}_{z}YZ_i^{(2)} + {}^{\mathrm{T}}_{z}YZ_i^{(2)} + {}^{\mathrm{B}}_{z}YZ_i^{(2)} \\ &+ {}^{\mathrm{A}}_{z}XZ_i^{(3)} + {}^{\mathrm{T}}_{z}XZ_i^{(3)} + {}^{\mathrm{B}}_{z}XZ_i^{(3)} + {}^{\mathrm{A}}_{z}YZ_i^{(4)} + {}^{\mathrm{T}}_{z}YZ_i^{(4)} + {}^{\mathrm{B}}_{z}YZ_i^{(4)}, \end{aligned} \tag{4}$$

which is the sum of forces along the Z-axis.

Considering next the rotational contributions, a beam under axial loading, which is simultaneously bent, gives rise to a buckling term which is again the product of a bending angle, θ, and an axial force component. For rotations about the Z-axis, this gives

$$\begin{aligned} W_i &= {}^{\mathrm{M}}_{w}XY_i^{(1)} + {}^{\mathrm{B}}_{w}XY_i^{(1)} + {}^{\mathrm{M}}_{w}XY_i^{(2)} + {}^{\mathrm{B}}_{w}XY_i^{(2)} \\ &+ {}^{\mathrm{M}}_{w}XY_i^{(3)} + {}^{\mathrm{B}}_{w}XY_i^{(3)} + {}^{\mathrm{M}}_{w}XY_i^{(4)} + {}^{\mathrm{B}}_{w}XY_i^{(4)}. \end{aligned} \quad (5)$$

For each beam in Eq. (5) there are two terms, one analogous to the non-buckling expression, and denoted with a superscript M, and one extra term, such as ${}^{\mathrm{B}}_{w}XY_i^{(1)}$, which is due to buckling. Similarly, we have

$$U_i = {}^{\mathrm{M}}_{u}XZ_i^{(1)} + {}^{\mathrm{B}}_{u}XZ_i^{(1)} + {}^{\mathrm{Q}}_{u}YY_i^{(2)} + {}^{\mathrm{M}}_{u}XZ_i^{(3)} + {}^{\mathrm{B}}_{u}XZ_i^{(3)} + {}^{\mathrm{Q}}_{u}YY_i^{(4)}, \quad (6)$$

for rotations about the Y-axis, and

$$V_i = {}^{\mathrm{Q}}_{v}XX_i^{(1)} + {}^{\mathrm{M}}_{v}YZ_i^{(2)} + {}^{\mathrm{B}}_{v}YZ_i^{(2)} + {}^{\mathrm{Q}}_{v}XX_i^{(3)} + {}^{\mathrm{M}}_{v}YZ_i^{(4)} + {}^{\mathrm{B}}_{v}YZ_i^{(4)}, \quad (7)$$

for rotations about the X-axis, where Q denotes the torque.

To study how thin sheets behave during fracture, the beams are assumed to have a rectangular cross-section. Resistance towards bending within the plane is then much larger than that which governs out-of-plane bending. In the present calculations the chosen width-to-thickness ratio is 10.

3 DISORDER

One of the great advantages of lattice models is the ease with which disorder can be included. In the present calculations systems with two different types of disorder are considered. The most practical way is to generate thresholds according to $t = r^D$, where r is a random number on $[0, 1]$ and t is the breaking threshold. Fracture may then be fully explored as a function of disorder simply by varying the magnitude of D. This way, small or large values of D correspond to weak or strong disorders, respectively [10]. The two types of distribution used are (i) $D > 0$, where the power-law is bounded above by a maximum threshold of one and has a tail towards zero, and (ii) $D < 0$, where the power-law is bounded below by a minimum threshold of one and has a tail towards infinity.

The role played by disorder is important. There exists a cross-over in disorder between, on the one hand, systems for which there is always a regime of stable crack growth and, on the other hand, systems for which crack growth is unstable, or conditionally stable, from the very beginning. In the beam model the regime of stable crack growth is observed for $D > 1$ and $D < -3$ [11], although, provided the size of the system is sufficiently large, stable crack growth can also be observed for smaller $D > 0$ [12]. It is within the two regimes $D > 1$ and $D < -3$, however, that the universal value of $\zeta = 0.86$, reported in Ref. [8], is observed. Presently we include two disorders, one in each regime, i.e., $D = 1$ and $D = -5$.

4 THE FRACTURE CRITERION

To study how buckling affects fracture in a two-dimensional structure which buckles out of the plane, an appropriate breaking criterion should be chosen. In lattice models this

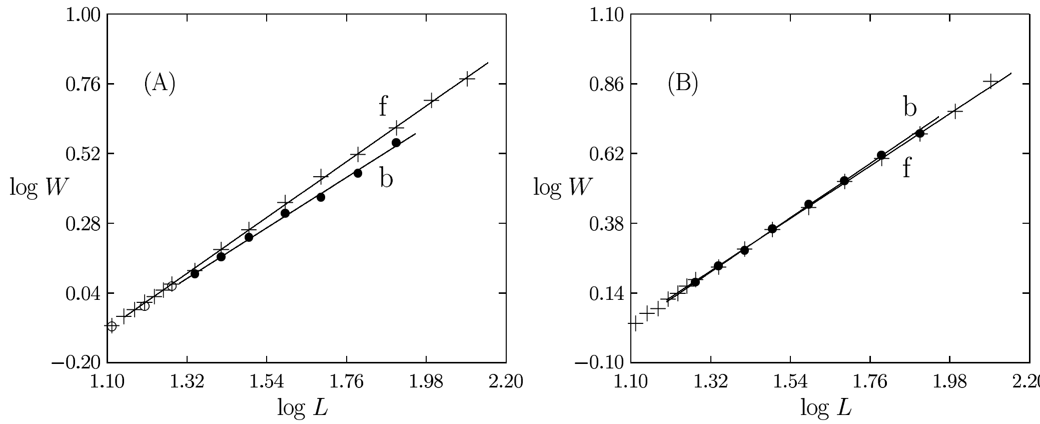

Figure 2: Log-log plots of the average roughness W as a function of the lattice size L, shown for (A) $D = 1$ and (B) $D = -5$. Non-buckling results (+) are denoted f and buckling results (•) are denoted b. In (A) the exponents are $\zeta_{\rm f} = 0.87(1)$ and $\zeta_{\rm b} = 0.79(2)$, and in (B) they are $\zeta_{\rm f} = 0.85(2)$ and $\zeta_{\rm b} = 0.86(2)$.

choice can be made quite freely, for instance it can be made to suit any specific engineering requirement. Often, however, the mode of rupture in the out-of-plane direction is radically different from that which takes place within the plane. In materials such as paper or cloth, for instance, the phenomenon which first springs to mind is tearing. The energy required to propagate a crack across a given area in this case is much less than that which causes the same area to fracture in a situation of pure tensile loading.

To emulate tearing on the meso-scale, the breaking rule chosen in our calculations combines the axial load on a beam with its torque, i.e., torque is assumed to increase the strain on a beam when it is under axial tensile loading. The larger the load, the more sensitive the beam will be to the presence of a specified amount of torque. In the case of a compressive load, on the other hand, strain is assumed to be alleviated by torque, but only to a very small degree.

5 RESULTS

Typically, in our simulations of a buckling lattice, fracture proceeds in a non-buckling manner until, suddenly, the stress-field which involves out-of-plane deflections becomes energetically favourable over the stress-field which would otherwise be confined within the plane. This usually happens when one of the developing cracks reaches a critical size. Different rules are then activated by which the crack propagates across the lattice, both in the sense of the stress-field being altered and in the sense of enabling beams to be broken in an out-of-plane deformation mode (tearing).

In Fig 2A the log-log values of W as a function of L are shown for $D = 1$. The roughness exponent is measured as the slope of the straight-line fit and is denoted "b" in the case of buckling and "f" (flat) otherwise. The exponent obtained for the buckling beam lattice is $\zeta = 0.79(2)$, a result which lies significantly below the non-buckling value of $\zeta = 0.87(1)$. The average number of beams broken is also reduced in this case. In other words the path taken to traverse the width of the sample is shortened, an effect which is due to the stress-field being intensified by out of plane deflections at the crack tip. The interplay between stress and quenched disorder in this case is thus shifted towards an earlier cross-over, i.e., from stable non-localized crack growth, where the typical length scale is infinite, to localized crack growth, characterized by finite length scales.

The result for $D = -5$ is shown in Fig. 2B. Here the roughness exponent obtained for the buckling lattice is marginally larger than the one obtained for the non-buckling lattice, i.e., $\zeta = 0.86(2)$ as opposed to $\zeta = 0.85(2)$, a difference, however, which is not significant, in contrast with the situation for $D = 1$. The average number of beams broken here is the same as in the non-buckling case. From the limited range of disorders included in the present study it would thus seem that buckling affects fracture in different ways according to the type of distribution used to generate disorder. In the case of $D = -5$, the intensified stress at the crack tip caused by out-of-plane deflections may not be sufficient to overcome obstacles in the path of the crack – obstacles which for $D < 0$ distributions are present in the form of unusually strong beams.

It remains to be seen whether or not this pattern persists for larger values of $|D|$. The result obtained for $D = 1$ is, in fact, consistent with the experimental result of $\zeta = 0.8$ for brittle fracture in three dimensions. The exponent obtained at $D = -5$ is not consistent with this, but may be a transitional result between localized and non-localized fracture. Indeed, as the tail towards infinitely strong beams increases for $D < -5$, the stress-strain response gradually attains a shape similar to that which characterizes the situation at $D > 1$ [11]. Further investigations into these matters are currently underway.

References

[1] See, e.g., *Statistical Models for the Fracture of Disordered Media*, edited by H.J. Herrmann and S. Roux (North-Holland, Amsterdam, 1990).

[2] L. de Arcangelis, S. Redner and H.J. Herrmann, J. Phys. Lett. (Paris) **46**, L585 (1985).

[3] S. Roux and E. Guyon, J. Phys. Lett. (Paris) **46**, L999 (1985).

[4] H.J. Herrmann, A. Hansen and S. Roux, Phys. Rev. B **39**, 637 (1989).

[5] A.L. Barabasi and H.E. Stanley, *Fractal Concepts in Surface Growth* (Cambridge University Press, Cambridge, 1990).

[6] J.Ø.H. Bakke, J. Bjelland, T. Ramstad, T. Stranden and A. Hansen, *To be published.*

[7] G.G. Batrouni and A. Hansen, Phys. Rev. Lett. **80**, 325 (1998).

[8] B. Skjetne, T. Helle and A. Hansen, Phys. Rev. Lett. **87**, 125503 (2001).

[9] R.J. Roark and W.C. Young, *Formulas for Stress and Strain* (McGraw-Hill, New York, 1975).

[10] A. Hansen, E.L. Hinrichsen and S. Roux, Phys. Rev. B **43**, 665 (1991).

[11] B. Skjetne, T. Helle and A. Hansen, *To be published.*

[12] S. Roux and A. Hansen, Europhys. Lett. **11**, 37 (1990).